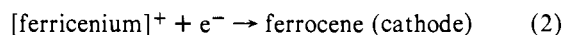
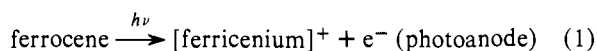


Figure 1. (a) Photocurrent against time in 0.1 M $[n\text{-Bu}_4\text{N}]\text{ClO}_4$ in CH_3CN (O) and $\text{C}_2\text{H}_5\text{OH}$ (●) for an n-type Ge electrode potentiostated at +0.29 V vs. SCE in CH_3CN and at +0.36 V vs. SCE in $\text{C}_2\text{H}_5\text{OH}$. In (b) the conditions are the same except that the solution contains 0.05 M ferrocene and enough ferricenium to bring the E_{redox} to +0.29 or +0.36 V vs. SCE in CH_3CN or $\text{C}_2\text{H}_5\text{OH}$, respectively.

completely effective hole capture by the ferrocene. Qualitatively, this is the sort of behavior found previously⁸ for n-type Si under the same conditions. The conclusion is that ferrocene can undergo one-electron oxidation to ferricenium in competition with oxidation of Ge.

The maintenance of a constant photocurrent in the presence of ferrocene/ferricenium indicates that the conversion of light to electricity can be sustained; the equations



reflect the redox chemistry occurring at the n-type Ge photoanode and Pt cathode, respectively. However, the photocurrent at short circuit is low; the observed quantum efficiency for electron flow is only $\sim 10^{-2}$ at 633 nm. Further, the open-circuit photopotential is only ~ 280 mV at the highest illumination intensities from the 514.5-nm output of our Ar ion laser (Figure 2). Thus, this photoelectrochemical cell is very inefficient as an optical energy conversion device.

The open-circuit potential data do provide some important information concerning the n-Ge interface energetics. The position of E_{redox} (ferricenium/ferrocene) in the experiment summarized in Figure 2 was 0.33 V vs. SCE. That is, at charge transfer equilibrium in the dark the n-Ge potential, E_f , is at 0.33 V vs. SCE. The light effect is such that the n-Ge potential moves more negative by ~ 280 mV on the electrochemical scale to ~ 0.1 V vs. SCE. Generally, the maximum open-circuit photopotential of an n-type semiconductor is close to the so-called flat-band potential, E_{FB} , where the bands are no longer bent.^{8,11,12} Since the heavily doped n-type material has a Fermi level, E_f , ~ 0.1 eV below the conduction band, the conduction band potential, E_{CB} , at the interface will be ~ 0.1 V more

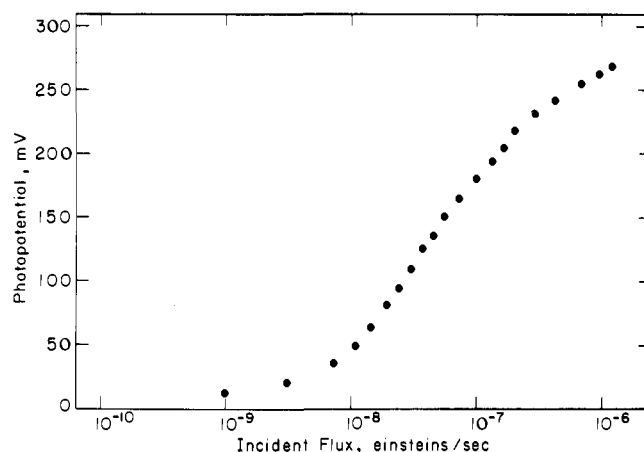
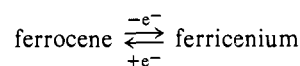


Figure 2. Photopotential between Pt and n-Ge under 514.5-nm laser irradiation (1.5-mm beam diameter). Electrolyte is $\text{C}_2\text{H}_5\text{OH}$ solution of ferrocene/ferricenium with 0.1 M $[n\text{-Bu}_4\text{N}]\text{ClO}_4$, at $E_{\text{redox}} = +0.33$ V vs. SCE. Same electrode as in Figure 1.

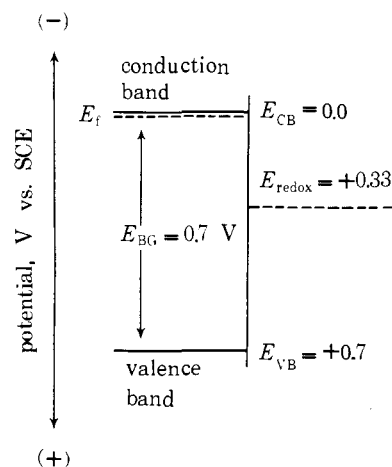
negative than E_{FB} . Scheme I summarizes the present situation assuming that the maximum photopotential of the n-Ge electrode brings it to E_{FB} . Thus, the interface position of E_{CB} and that for the valence band, E_{VB} , are located in a crude fashion on the electrochemical scale. In comparing Scheme I with the same data⁸ for n-type Si ($E_{\text{BG}} = 1.1$ eV),¹³ we note that the E_{CB} position is more positive for n-Ge, while the E_{VB} positions are nearly the same.

The cyclic voltammetry of an n-type Ge electrode exposed to a $\text{CH}_3\text{CN}/0.1$ M $[n\text{-Bu}_4\text{N}]\text{ClO}_4$ solution of ferrocene has been studied. Cyclic voltammetric scans are shown in Figures 3 and 4. First, under low-level illumination (633 nm, ~ 6 mW) or even in total darkness we observe oxidation and reduction waves corresponding to the



system. Quite interestingly, the waves are in nearly the same position as for a Pt working electrode;¹⁴ the peak to peak separation is rather small (~ 85 mV); and even fairly high scan rates do not give too large a shift in the position of either peak. The scan rate dependence of the peak current is as expected for a reversible solution couple.¹⁵ These results show that n-Ge is not blocking to the oxidation of ferrocene; indeed, the behavior is such that the n-Ge is nearly reversible for the redox system. These results are quite different compared to n-Si where little dark anodic current passes corresponding to ferrocene oxidation. The difference between n-Si and n-Ge can

Scheme I



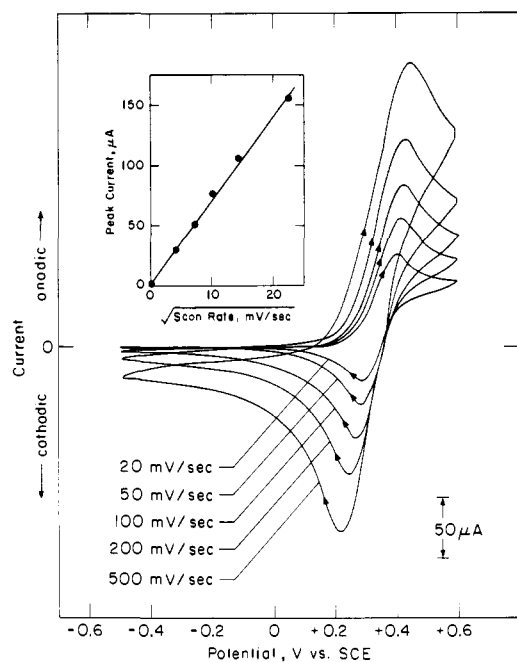


Figure 3. Cyclic voltammograms for freshly HF-etched n-Ge electrode (same as in Figure 1), in unstirred 7.5×10^{-3} M ferrocene with 0.1 M $[n\text{-Bu}_4\text{N}]\text{ClO}_4$ in CH_3CN solution. Uniform irradiation at 6 mW of 632.8-nm light. Inset shows that peak current is proportional to square root of scan rate, as expected for electroactive species in solution.

be attributed to a number of possible factors including electron injection into the more accessible conduction band, electron tunneling through the thinner barrier, and surface states. Experiments are underway to assess the relative contributions of these mechanisms of interfacial charge transfer.

For n-Si, photoanodic current obtains when holes, h^+ , are generated in the valence band. These unfilled states apparently do overlap very effectively with the ferrocene levels and the photoinduced oxidation is effected. At sufficiently high illumination, oxidation via photogenerated holes in n-Ge is possible (Figure 4). Further, note that the oxidation current onsets at a ~ 200 mV more negative potential and peaks at a more negative potential than in the dark. This is consistent with the measured open-circuit potential of ~ 280 mV and is in accord with the notion that oxidation via holes in the valence band can begin to occur at electrode potentials more positive than E_{FB} , even if such oxidation is contrathermodynamic, i.e., the photoanodic current flow onsets at a more negative potential than at a reversible electrode in the dark. For n-Ge the quantum yield for electron flow at short-circuit ($\text{Ge potential} = E_{\text{redox}}$) or at Ge potentials more negative than E_{redox} is low owing to the ready reduction of ferricenium at those same potentials (Figures 3 and 4).

B. Characterization of Derivatized Electrodes by Cyclic Voltammetry. n-Type Ge derivatized with I or II by the procedure outlined in the Experimental Section has been characterized by cyclic voltammetry in $\text{C}_2\text{H}_5\text{OH}$ or CH_3CN solutions of 0.1 M $[n\text{-Bu}_4\text{N}]\text{ClO}_4$. Results with either I or II are roughly the same and examples will be given for each.

Figure 5 shows the cyclic voltammetry results for an n-type Ge electrode derivatized with I. First, it is noteworthy that we see cyclic waves at all; for a nonderivatized electrode under the same conditions anodic currents can be seen but there is no peak and there is typically little or no cathodic current. As shown in Figure 5 we do find that the derivatized electrode does exhibit anodic and cathodic peaks in the *dark* at a potential of ~ 0.5 V vs. SCE. With intense illumination, however, the peaks sharpen and are up to ~ 200 mV more negative. Figure

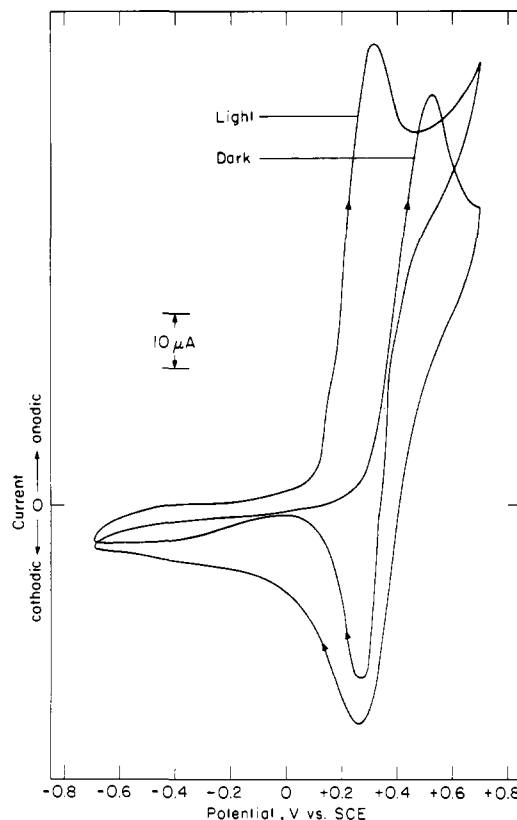


Figure 4. Cyclic voltammograms for freshly HF-etched n-Ge in unstirred CH_3CN solution of 0.1 M $[n\text{-Bu}_4\text{N}]\text{ClO}_4$ and 2×10^{-3} M ferrocene. Scans recorded at 200 mV/s; light refers to ~ 262 -mW irradiation with 488-nm laser light (1.5-mm diameter beam).

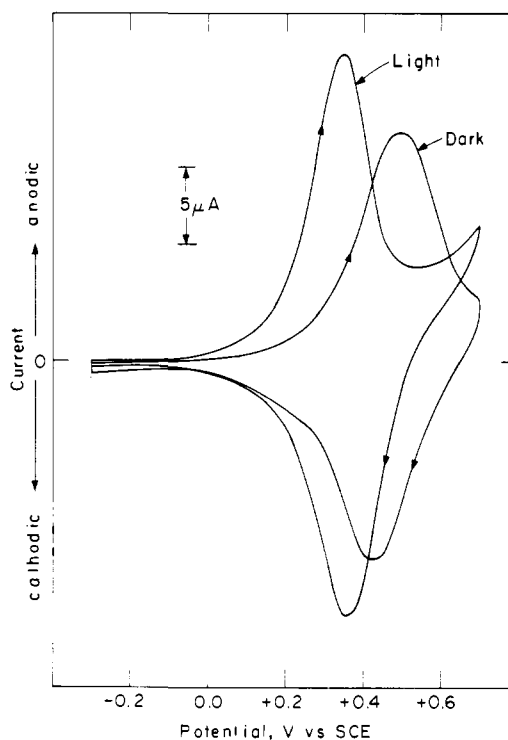


Figure 5. Cyclic voltammograms for n-Ge derivatized with I in stirred 0.1 M $[n\text{-Bu}_4\text{N}]\text{ClO}_4/\text{CH}_3\text{CN}$. Electrode had been derivatized by 3-h immersion in a solution of 8.3×10^{-3} M I in isooctane at 298 K. Scan rate is 100 mV/s, light here refers to ~ 120 mW laser irradiation at 514.5 nm (1.5-mm diameter beam).

6 shows the cyclic voltammetric wave as a function of scan rate. Up to rates of 200 mV/s the peak current is directly propor-

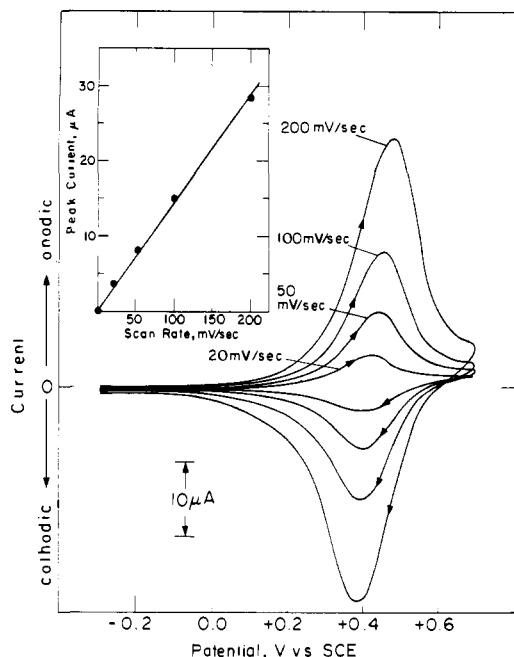


Figure 6. Cyclic voltammograms for electrode in Figure 5 as a function of scan rate at low level irradiation. Inset shows a linear dependence of peak current on scan rate.

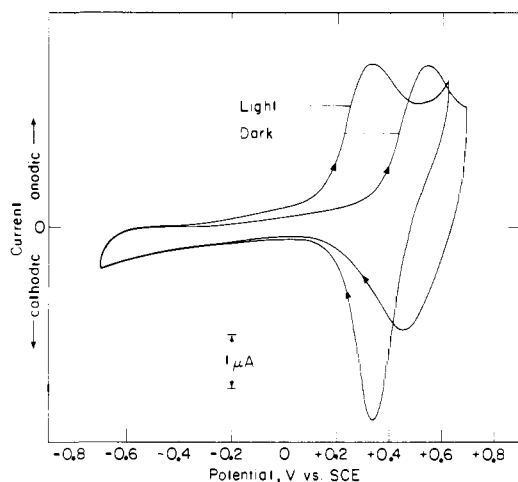


Figure 7. Cyclic voltammograms for n-Ge derivatized with II in unstirred 0.1 M $[n\text{-Bu}_4\text{N}]\text{ClO}_4/\text{CH}_3\text{CN}$ in the dark, and under $\sim 291\text{-mW}$ irradiation at 488 nm (1.5-mm laser beam diameter). Scan rate = 100 mV/s. Electrode had been derivatized by 6 h immersion in a solution of 0.093 M II in isooctane.

tional to scan rate, as expected for a surface-bound reversible couple.¹⁶ Figures 7–9 give comparable data for the n-type Ge derived with II. Figures 7 and 8 show a comparison of the behavior in $\text{C}_2\text{H}_5\text{OH}$ vs. CH_3CN solution. Qualitatively, the results for derivatization with I and II are thus established to be quite similar.

One additional important piece of information is given by the cyclic voltammetric scans in Figure 8. The dark cathodic return peak associated with the photooxidized species is at the same potential as when the oxidation is carried out in the dark. That is, with the light on the oxidation wave is at ~ 0.3 V vs. SCE; at a potential ~ 0.7 V vs. SCE the light is switched off and the reduction peak is found to be at a more positive potential than when the light is on.

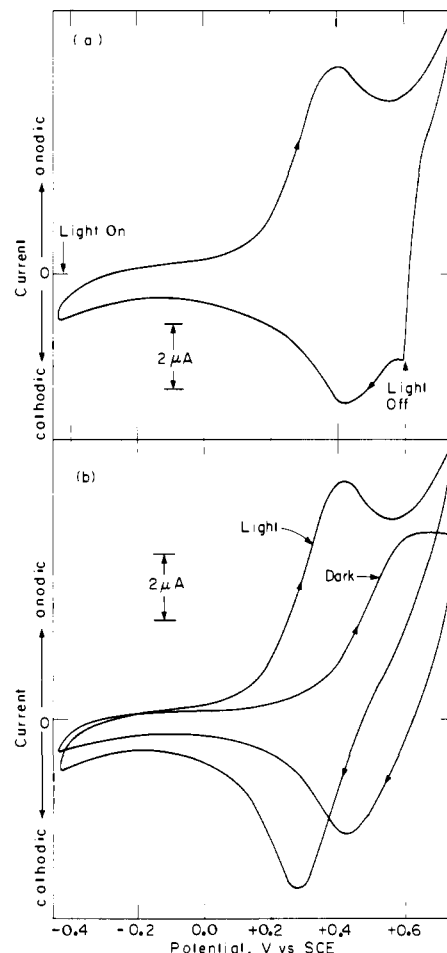


Figure 8. Cyclic voltammograms of n-Ge derivatized with II in unstirred 0.1 M $[n\text{-Bu}_4\text{N}]\text{ClO}_4/\text{C}_2\text{H}_5\text{OH}$ in dark, and under $\sim 210\text{-mW}$ laser irradiation at 514.5 nm (1.5 mm beam diameter). Electrode had been derivatized for 2 h in ~ 0.083 M isooctane solution of II. Scan rate = 500 mV/s. Part (a) shows light oxidation and dark reduction waves; part (b) shows voltammograms run entirely in the dark and under laser irradiation, respectively.

The data given in Figures 5–8 have been reproduced a number of times without major qualitative changes. However, peak potentials and surface coverages (as determined by integrated area under the cyclic waves) do vary from experiment to experiment. Coverage of electroactive material is typically in the range of 3×10^{-10} to 5×10^{-9} mol/cm². Such electroactive material is persistently attached; Figure 10 shows that relatively minor changes in the cyclic waves obtain after hundreds of cycles between two potential limits. Comparable durability can be obtained in $\text{C}_2\text{H}_5\text{OH}$ solution. However, in either solution, gross changes do result when the potential range is too anodic. A “safe” range is typically -1.5 to $+0.8$ V vs. SCE.

Summary

This work establishes the persistent attachment of electroactive ferrocene derivatives to the surface of n-type Ge photoelectrodes. Intense illumination of the electrode shows that the oxidation can be carried out at an underpotential of ~ 200 mV, and photoassisted oxidations using band gap, or greater, energy light can be envisioned. Potential substrates are those which are oxidizable with ferricenium. The interfacial energetics for n-type Ge are such that the positions of the conduction and valence band edges are at 0.0 and $+0.7$ V vs. SCE, respectively, in CH_3CN or $\text{C}_2\text{H}_5\text{OH}$ solutions of 0.1 M $[n\text{-}$

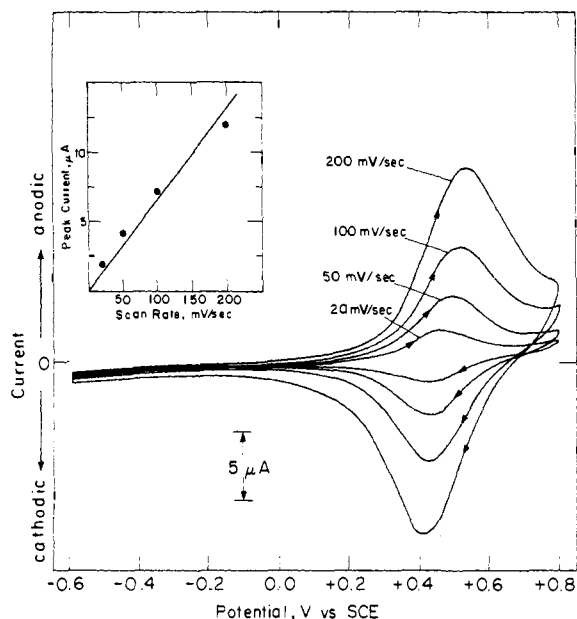


Figure 9. Cyclic voltammograms of *n*-Ge derivatized with II in unstirred 0.1 M $[n\text{-Bu}_4\text{N}]\text{ClO}_4/\text{CH}_3\text{CN}$, under 4-mW uniform irradiation at 632.8 nm (0.8-mm laser beam diameter, 6 \times expanded). Electrode had been derivatized by 4.3-h immersion in 0.16 M solution of II in isooctane at 298 K. Inset shows that peak current is directly proportional to scan rate, as expected for surface-bound electroactive species.

$\text{Bu}_4\text{N}]\text{ClO}_4$ and ferricenium/ferrocene. The energetics of the *n*-Ge and ferricenium/ferrocene system are essentially independent of whether the ferricenium/ferrocene system is surface attached. The ferricenium/ferrocene system appears to be nearly reversible, even in the dark, at *n*-type Ge and the reasons for this are currently under study.

Experimental Section

Materials. Antimony-doped *n*-type single-crystal Ge wafers (0.5 mm thick, 111 face) were obtained from Texas Materials Laboratory (Austin, Texas). Four-point probe measurements indicated a resistivity of approximately 10^{-2} ohm cm. Ferrocene, absolute $\text{C}_2\text{H}_5\text{OH}$, and spectrograde solvents were used as received from commercial sources. Ferricenium as the PF_6^- salt was prepared according to the literature,¹⁷ and derivatizing reagents I and II were synthesized as previously reported.^{4,9} $[n\text{-Bu}_4\text{N}]\text{ClO}_4$ was prepared by metathesis of the Br^- salt, and was recrystallized from CH_3OH .

Electrode Preparation. Germanium electrodes (~ 0.3 cm²) were fabricated by our usual method.^{8,11} Satisfactory electrical contacts were made by rubbing Ga-In eutectic on the back face of the crystal and mounting (with conducting silver epoxy) onto a coiled copper wire. The copper wire lead was ensheathed in a glass rod, and the assembly was insulated with ordinary epoxy to leave only the Ge crystal exposed to the electrolyte.

Before derivatization, the electrodes were first pretreated by anodization at +1.0 V vs. SCE in ~ 6 M H_2SO_4 for 30 s. This procedure presumably introduces functional groups on the electrode surface which can react with the derivatizing agents.⁷ During anodization, total currents of approximately $0.5\text{--}10.0 \times 10^{-2}$ C were passed, but since 6 M H_2SO_4 etches the Ge surface, this figure cannot be precisely correlated with the degree of surface functionalization introduced. Finally, the electrode was usually irradiated with 5 mW of uniform 632.8-nm laser light during anodization, but this was not found to be essential to successful subsequent derivatization.

Following this pretreatment, the electrodes were rinsed with distilled water and with acetone and air dried. They were then brought into a drybox with an inert atmosphere, and immersed in Ar-purged isooctane solutions of derivatizing agents I or II at 298 K. The concentrations of the derivatizing solutions were determined by UV-visible spectroscopy of suitably diluted aliquots, and were found to range between ~ 5 mM and fully saturated (>0.1 M). The derivatization proceeded for periods of 1–6 h, during which time the solutions were

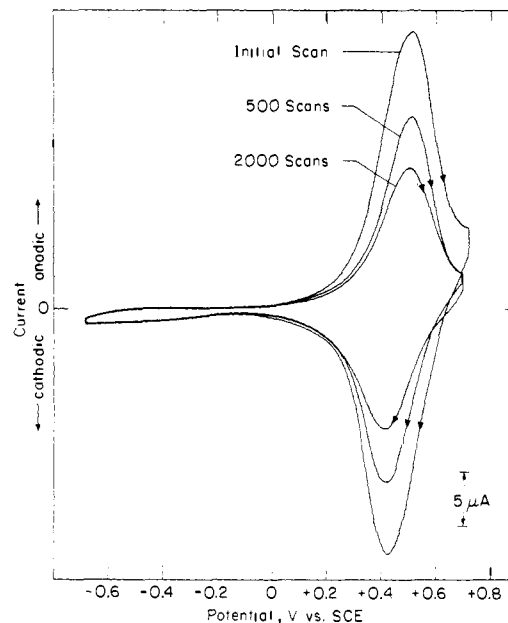


Figure 10. Cyclic voltammograms for *n*-Ge derivatized with I in unstirred 0.1 M $[n\text{-Bu}_4\text{N}]\text{ClO}_4/\text{CH}_3\text{CN}$; uniform irradiation at 4 mW of 632.8-nm laser light (0.8-mm beam diameter, 6 \times expanded). All scans performed at 200 mV/s; the electrode was cycled at this rate between +0.2 and +0.7 V vs. SCE the indicated number of times, and the lower potential limit was changed for the recorded scans. The electrode had been derivatized by 3.5-h immersion in an isooctane solution of I, ~ 0.03 M.

under inert atmosphere. The precise duration of derivatization was not a crucial consideration, although immersion times of only a few minutes—particularly in the more dilute solutions—gave low surface coverages, as determined from the integrated peak areas of the cyclic voltammograms.

After derivatization, the electrodes were swirled in isooctane and then in CH_3CN and air dried prior to use in electrochemical cells.

Electrochemical Characterization. All experiments were performed in single-compartment Pyrex vessels, equipped with saturated calomel (SCE) reference electrode, Pt gauze ($\sim 1 \times 3$ cm) counterelectrode, and Ge photoanode. In all cases, the supporting electrolyte was 0.1 M $[n\text{-Bu}_4\text{N}]\text{ClO}_4$, and the solvent either CH_3CN or absolute $\text{C}_2\text{H}_5\text{OH}$, at 298 K. For experiments with nonderivatized electrodes when ferrocene and/or ferricenium was added to the electrolyte, the solution E_{redox} was measured with a digital voltmeter. For such experiments the Ge electrode was etched for 15 s in concentrated HF at 298 K immediately prior to use. It was then rinsed with distilled H_2O and acetone and dried in air.

Cyclic voltammograms were obtained with a PAR 173 potentiostat equipped with a Model 179 coulometer, and operated in conjunction with a Model 175 voltage programmer. The voltammograms were recorded on a Houston Instruments XY recorder, but for the photocurrent vs. time plots shown in Figure 1, the current was continuously monitored on a strip chart recorder.

Illumination at 488 and 514.5 nm was provided by a Spectra Physics Ar ion laser (1.5-mm beam diameter). Irradiations at 632.8 nm were performed using either of two He-Ne lasers, Spectra Physics or Coherent Radiation, at 4 or 6 mW, respectively. Light intensity was varied with colored glass filters, and monitored with a beam splitter and a Tektronix J16 digital radiometer with J6502 probe.

Acknowledgment. We thank the U.S. Department of Energy, Office of Basic Energy Sciences, for support of this work. M.S.W. acknowledges support as a Dreyfus Teacher-Scholar Grant recipient, 1975–1980.

References and Notes

- (1) A. J. Bard and M. S. Wrighton, *J. Electrochem. Soc.*, **124**, 1706 (1977).
- (2) (a) H. Gerischer, *J. Electroanal. Chem.*, **82**, 133 (1977); (b) H. Gerischer and W. Mindt, *Electrochim. Acta*, **13**, 1329 (1968).
- (3) R. Memming, *J. Electrochem. Soc.*, **125**, 117 (1978).
- (4) M. S. Wrighton, R. G. Austin, A. B. Bocarsly, J. M. Bolts, O. Haas, K. D. Legg,

- L. Nadjó, and M. C. Palazzotto, *J. Am. Chem. Soc.*, **100**, 1602 (1978).
- (5) J. I. Pankove, "Optical Processes in Semiconductors", Dover Publications, New York, N.Y., 1971.
- (6) (a) W. Brattain and C. Garrett, *Bell Syst. Tech. J.*, **34**, 129 (1955); (b) D. Turner, *J. Electrochem. Soc.*, **103**, 252 (1956); (c) A. Uhler, *Bell Syst. Tech. J.*, **35**, 333 (1956); (d) R. Gereth and M. Cowher, *J. Electrochem. Soc.*, **115**, 645 (1968); (e) F. Beck and H. Gerischer, *Ber. Bunsenges. Phys. Chem.*, **63**, 500 (1959); (f) H. Gerischer, A. Mauerer, and W. Mindt, *Surf. Sci.*, **4**, 431 (1966).
- (7) (a) F. Beck and H. Gerischer, *Ber. Bunsenges. Phys. Chem.*, **63**, 943 (1959); (b) Y. Pleskov and B. Kabanov, *Dokl. Akad. Nauk SSSR*, **123**, 884 (1958); (c) E. Eflmov and I. Erusalimchik, *Russ. J. Phys. Chem. (Engl. Transl.)*, **35**, 266 (1961); (d) H. Gerischer and F. Beck, *Z. Phys. Chem. (Frankfurt am Main)*, **13**, 389 (1957); (e) R. Memming and F. Mollers, *Ber. Bunsenges. Phys. Chem.*, **76**, 609 (1972).
- (8) K. D. Legg, A. B. Ellis, J. M. Bolts, and M. S. Wrighton, *Proc. Natl. Acad. Sci. U.S.A.*, **74**, 4116 (1977).
- (9) M. S. Wrighton, R. G. Austin, A. B. Bocarsly, J. M. Bolts, O. Haas, K. D. Legg, L. Nadjó, and M. C. Palazzotto, *J. Electroanal. Chem.*, **87**, 429 (1977), and results submitted for publication.
- (10) (a) J. R. Lenhard and R. W. Murray, *J. Electroanal. Chem.*, **78**, 195 (1977); (b) P. R. Moses and R. W. Murray, *J. Am. Chem. Soc.*, **98**, 7435 (1976); (c) C. M. Elliott and R. W. Murray, *Anal. Chem.*, **48**, 1247 (1976); (d) D. G. David and R. W. Murray, *ibid.*, **49**, 194 (1977); (e) P. R. Moses, L. Wier, and R. W. Murray, *ibid.*, **47**, 1882 (1975); (f) J. C. Lennox and R. W. Murray, *J. Electroanal. Chem.*, **78**, 395 (1977); (g) B. E. Firth, L. L. Miller, M. Mitani, T. Rogers, J. Lennox, and R. W. Murray, *J. Am. Chem. Soc.*, **98**, 8271 (1976); (h) B. E. Firth and L. L. Miller, *ibid.*, **98**, 8273 (1976); (i) R. J. Burt, G. J. Leigh, and C. J. Pickett, *J. Chem. Soc., Chem. Commun.*, 940 (1976); (j) M. Fujihira, T. Matsue, and T. Osa, *Chem. Lett.*, 875 (1976); (k) T. Osa and M. Fujihira, *Nature (London)*, **264**, 349 (1976); (l) M. Fujihira, A. Tamura, and T. Osa, *Chem. Lett.*, 361 (1977); (m) N. R. Armstrong, A. W. C. Lin, M. Fujihira, and T. Kuwana, *Anal. Chem.*, **48**, 741 (1976); (n) J. F. Evans, T. Kuwana, M. T. Henne, and G. P. Royer, *J. Electroanal. Chem.*, **80**, 409 (1977); (o) A. Diaz, *J. Am. Chem. Soc.*, **99**, 5838 (1977); (p) A. F. Diaz, U. Hetzler, and E. Kay, *ibid.*, **99**, 6780 (1977); (q) M. Fujihira, N. Ohishi, and T. Osa, *Nature (London)*, **268**, 226 (1977).
- (11) H. Gerischer, *J. Electroanal. Chem.*, **56**, 263 (1975).
- (12) (a) A. B. Ellis, S. W. Kaiser, J. M. Bolts, and M. S. Wrighton, *J. Am. Chem. Soc.*, **99**, 2839 (1977); (b) A. B. Ellis, J. M. Bolts, S. W. Kaiser, and M. S. Wrighton, *ibid.*, **99**, 2848 (1977); (c) A. B. Ellis, J. M. Bolts, and M. S. Wrighton, *J. Electrochem. Soc.*, **124**, 1603 (1977); (d) J. M. Bolts, A. B. Ellis, K. D. Legg, and M. S. Wrighton, *J. Am. Chem. Soc.*, **99**, 4826 (1977).
- (13) H. F. Wolf, "Silicon Semiconductor Data", Pergamon Press, Oxford, 1969, p 111.
- (14) G. J. Janz and R. P. T. Tomkins, "Nonaqueous Electrolytes Handbook", Vol. II, Academic Press, New York, N.Y., 1973, and references cited therein.
- (15) R. S. Nicholson and I. Shain, *Anal. Chem.*, **36**, 706 (1964), and references cited therein.
- (16) E. Laviron, *J. Electroanal. Chem.*, **39**, 1 (1972).
- (17) D. N. Hendrickson, Y. S. Sohn, and H. B. Gray, *Inorg. Chem.*, **10**, 1559 (1971).

Infrared Circular Dichroism Associated with the OH-Stretching Vibration in the Methyl Ester of Mandelic Acid

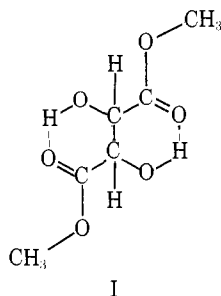
Curtis Marcott, Carol C. Blackburn, Thomas R. Faulkner, Albert Moscovitz,* and John Overend*

Contribution from the Department of Chemistry, University of Minnesota, Minneapolis, Minnesota 55455. Received December 19, 1977

Abstract: The infrared circular dichroism (CD) spectrum associated with the OH-stretching vibration in methyl mandelate has been measured. The methyl mandelate CD results suggest a new interpretation of the CD spectrum of dimethyl tartrate.

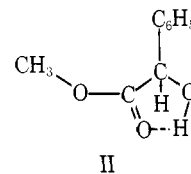
Introduction

Experimental observation of circular dichroism (CD) associated with the CH-stretching vibrations in tartaric acid was recently reported by Sugeta et al.¹ Their results indicate that bisignate contributions to the spectra are not evident; hence, that the coupled-oscillator contribution arising from the coupling of the symmetric and antisymmetric stretching modes is negligible.^{1,2} Keiderling and Stephens recently reported observing a bisignate spectrum in the OH-stretching region of *d*-dimethyl tartrate, [-CH(OH)COOCH₃]₂ (I), which they



interpreted on the basis of a coupled-oscillator calculation that agreed qualitatively with the observed spectrum.³

In the present study measurements of vibrational CD associated with the single OH stretch in *d*-, *l*-, and *dl*-methyl mandelate, [PhCH(OH)COOCH₃] (II), have been made.



Methyl mandelate is structurally related to dimethyl tartrate but the interpretation of the vibrational CD spectrum should be more straightforward since it contains only one OH group and there is no possibility of a degenerate coupled-oscillator contribution to the rotational strength associated with the OH-stretching vibration. The results of the methyl mandelate study have important implications in the interpretation of the CD spectrum of dimethyl tartrate.

Experimental Section

The methyl mandelate samples used in this work were prepared by esterification of mandelic acid samples obtained from the Aldrich Chemical Co. The mandelic acid was dissolved in methanol and refluxed with ~5% concentrated sulfuric acid for 1 h. The product was mixed with H₂O and ether and enough Na₂CO₃ was added to bring the pH to about 3. The water layer was extracted several times and the ether evaporated. The product was dried over CaSO₄ and recrystallized from hot petroleum ether. [α]_D values of +170.5 and -168.8° (c 1.000, CHCl₃) were observed for the *d* and *l* enantiomers, respectively.

Infrared CD measurements were made on the Holzwarth-Chabay